Analysis and Design of Integrated Active Circulator Antennas

Christos Kalialakis, Martin J. Cryan, *Member, IEEE*, Peter S. Hall, *Senior Member, IEEE*, and Peter Gardner, *Member, IEEE*

***Abstract*—A study on the analysis and design of active integrated antennas based on active quasi-circulators is reported in this paper. The antenna consists of a novel hybrid active circulator and a short-circuited quarter-wavelength microstrip antenna, which combine to form an active antenna with transmit and receive action at the same frequency. A full-wave model of the configuration using the extended finite-difference time-domain method is devised to analyze its operation, to study parasitic electromagnetic coupling effects, and to derive design guidelines. Experimental results for a hybrid model are also presented.**

***Index Terms*—Active antennas, diplexers, FDTD methods, microstrip antennas, microwave circulators.**

I. Introduction

ACTIVE integrated antennas involve the intimate integration of active devices and antennas. These modules are potentially attractive as lightweight and low-cost solutions for potential uses in high-volume millimetric-wave systems. A multitude of active antennas have appeared in the literature based on various combinations of radiators with amplifiers, mixers, and oscillators [1]. Configurations have also been suggested that exhibit transmit–receive operation. The key issue for these transceivers is the isolation between the transmit and receive ports. Isolation can be achieved by using either inherent properties of microstrip antennas [2] or auxiliary circuits incorporating unilateral devices. In this paper, the latter approach is adopted by using an active quasi-circulator.

The analysis of active integrated antennas is a demanding task. Fringing fields always create undesirable coupling between compactly arranged circuit elements, active devices, and radiators. An additional factor to be dealt with is the nonlinear nature of active devices, which can generate harmonics [3]. Methods depending on separating the active devices from the antennas do not take into account the coupling. It is clear that a method that combines the ability to handle antennas and circuits concurrently is the optimal solution [1]. The most promising candidate is the finite-difference time-domain (FDTD) method as extended to include circuit elements [4], [5]. Few works using the extended FDTD method to analyze active antennas have appeared in the literature [6], [7].

Manuscript received March 18, 1999.

C. Kalialakis, P. S. Hall, and P. Gardner are with the Communications Engineering Research Group, School of Electronic and Electrical Engineering, The University of Birmingham, Birmingham B15 2TT, U.K. (e-mail: p.gardner@bham.ac.uk).

M. J. Cryan is with the Department of Electronic and Information Engineering, University of Perugia, Perugia I-06125, Italy.

Publisher Item Identifier S 0018-9480(00)04666-4.

In Section II, the initial design procedure for a version of the active quasi-circulator antenna, based on 100-Ω variable gain blocks, is described. The FDTD analysis of two versions of the resulting structure, one with the antenna outside the ring of the circulator and one with it inside, is described in Section III. The differences between these two versions help to show the effects of the close coupling between circuit and antenna in the latter, and field plots produced using FDTD help to reveal the details of the coupling.

Sections IV and V describe the design and experimental evaluation of a practical version of the integrated active antenna circulator. This uses commercially available packaged monolithic-microwave integrated-circuit (MMIC) gain blocks with nominal 50-Ω port impedances at normal bias. The simulation of the design was carried out using a circuit simulator. To achieve the necessary impedance transformations in distributed matching networks within the circulator required a wide range of microstrip linewidths, making it impractical to simulate the 50-Ω gain-block-based structure in FDTD with a sufficiently small mesh size. However, a comparison of the experimental results of Section V and the FDTD results of Section III reveal the same qualitative features, demonstrating the power of FDTD in identifying coupling phenomena in tightly integrated structures. A detailed quantitative comparison would require either a significant increase in computation speeds, to make possible the FDTD analysis of the experimental model, or the availability of variable-gain 100-Ω MMIC gain blocks, to make it possible to realize experimentally the 100-Ω gain-block version.

Section VI describes the FDTD calculations of the radiation patterns for the 100-Ω version of the module and the measured results for the radiation patterns of the 50-Ω version. Section VII describes several further calculations using the FDTD method, performed to determine quantitatively the effects of the antenna topology on the performance of the module.

II. Design Based on 100-Ω Gain Blocks

A. Principle of Circulator Operation

A circulator is, in general, a three-port device in which signals pass from one port to another in one direction only. They are used to separate transmit and receive paths in communication systems or radars. Active circulators have drawn considerable interest with their advantages of size and weight over conventional ferrite devices [8], [9].

Our active circulator utilizes three gain blocks connected in a ring arrangement (Fig. 1). There are two signal paths from

0018–9480/00$10.00 © 2000 IEEE

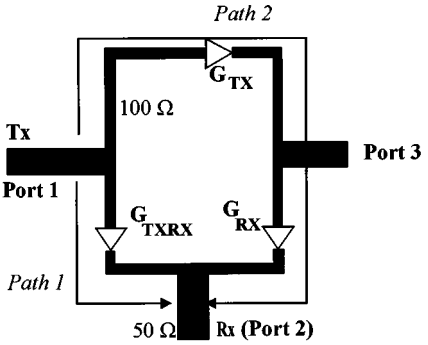

Fig. 1. Metal-surface layout of a planar active circulator based on 100-Ω gain blocks.

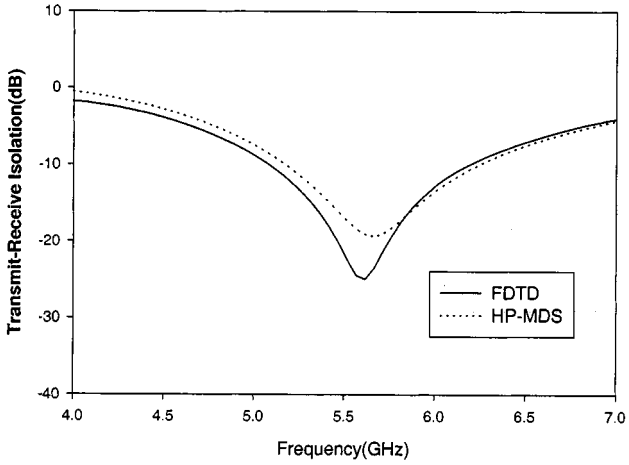

Fig. 2. Transmit–receive isolation (S_{21}) for a 100-Ω active circulator (FDTD versus HP-MDS).

the transmitter (port 1) to the receiver (port 2). The paths are labeled 1 and 2 in Fig. 1. By adjusting the phase lengths of the two paths and the gains, *phase cancellation* occurs at the receiver to create the quasi-circulation (or diplexing action). Specifically, the condition is that the power arriving at the receiver from the two possible paths is of equal magnitude and the phase difference of the two paths is 180°.

B. Circulator Design

The circulator was designed using the Hewlett-Packard Microwave Design System (HP-MDS) software, allowing for optimization of the amplifier gains and the lengths of the transmission lines in order to obtain the desired isolation. The choice of the impedance for gain blocks dictates the matching requirements. For the initial design exercise described here, 100-Ω gain blocks are used to avoid matching difficulties and to make the layout simpler and more amenable to FDTD analysis (Fig. 1). Such gain blocks can be implemented in MMIC technology, another attractive feature of active circulators [9].

III. FDTD Analysis of the Active Integrated Circulator Antenna Using 100-Ω Gain Blocks

A. FDTD Modeling of Gain Block

In order to simulate the circulator, gain blocks must be incorporated in FDTD. Transistors introduce certain difficulties because of their unilateral nature and the fact they are two-port devices. In our code, a linear gain block was incorporated by realizing the input and output ports in separate cells. At the input port, a resistor equal to the input impedance is realized. At the output port, the dependent voltage source is modeled in series with the desired output resistor, i.e., like a resistive voltage source [5]

$$E_z^{n+1} = \frac{2R_{\text{out}} \cdot \varepsilon \cdot \Delta x \cdot \Delta y - \Delta t \cdot \Delta z}{2R_{\text{out}} \cdot \varepsilon \cdot \Delta x \cdot \Delta y + \Delta t \cdot \Delta z} E_z^n + \frac{2R_{\text{out}} \cdot \Delta x \cdot \Delta y \cdot \Delta t}{2R_{\text{out}} \cdot \varepsilon \cdot \Delta x \cdot \Delta y + \Delta t \cdot \Delta z} (\nabla \times \bar{H})_z^{n+1/2} - \frac{2 \cdot \Delta t \cdot A \cdot \Delta z \cdot E_{\text{in}}^{n+1}}{2R_{\text{out}} \cdot \varepsilon \cdot \Delta x \cdot \Delta y + \Delta t \cdot \Delta z} \quad (1)$$

where E_{in}^{n+1} is the value of the electric field calculated at the input node, A is the internal gain of the block, and R_{out} is the output impedance of the gain block. The distance between the input and output port was dictated by the size of a physical gain block (2-mm linear dimensions). Embedding the ideal gain block in the FDTD space resulted in isolation (S_{12}) of more than 20 dB. This is a reasonable value for a practical gain block, and agreed well with HP-MDS simulations of a gain block in which the dominant physical feedback mechanism is the electromagnetic coupling across the space occupied by the device. A more complex FDTD model of the gain block would include a detailed equivalent-circuit representation of all the feedback mechanisms. However, for an initial assessment of the module design, the simple model provided an effective approximation to the isolation of a typical transistor.

In the FDTD model, short-circuit pins are modeled as wires by forcing the tangential electric field to be zero along the direction of the wire. The same approach is followed for the modeling of the metal plates of zero thickness, in accordance with the usual procedure for microstrip structures [11].

B. 100-Ω Active Circulator—FDTD and MDS Results

The dimensions of the 100-Ω hybrid circuit (dielectric constant $\varepsilon_r = 2.2$, thickness $h = 1.1$ mm) are 12 × 19.1 mm, with the 50- and 100-Ω lines having widths 3.3 and 0.9 mm, respectively. The gains are $G_{\text{TXRX}} = 1$, $G_{\text{TX}} = 1$, $G_{\text{RX}} = 1.8$ (linear units). The structure was then simulated using our extended three-dimensional (3-D) FDTD program by using $151 \times 151 \times 51$ cells with $\Delta x = 0.3$ mm, $\Delta y = 0.3$ mm, and $\Delta z = 0.37$ mm. From our experience, at least three cells across the microstrip linewidth and through the substrate thickness are required to get accurate results. Wide-band information can be retrieved from FDTD using a Gaussian pulse as excitation and performing Fourier transforms of the transients. First- and second-order Mur absorbing conditions were used to truncate the computational domain [12]. Good agreement was obtained for the transmit–receive isolation (Fig. 2) between HP-MDS and FDTD. The difference is attributed to frequency-independent gain blocks used in the MDS design. FDTD can also provide valuable information on the physics of the circuit. The spatial distribution of the electric field just underneath the metal layout

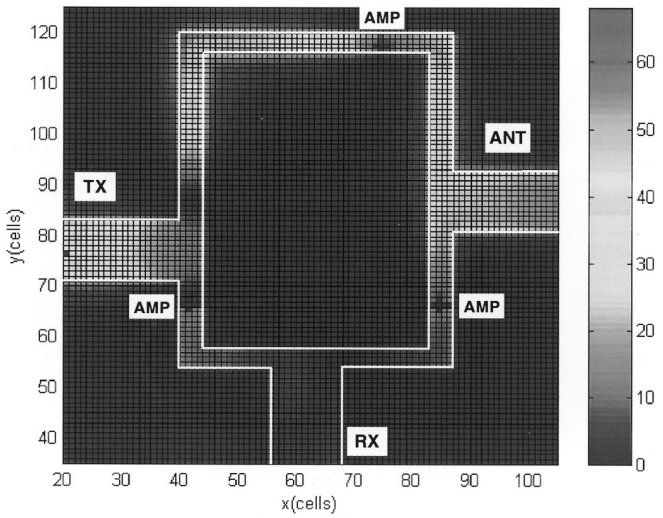

Fig. 3. Distribution of the normal electric-field magnitude on the surface for the active circulator (100 Ω) at the maximum isolation frequency (calculated using FDTD). The space between white lines is metal and the rest is dielectric.

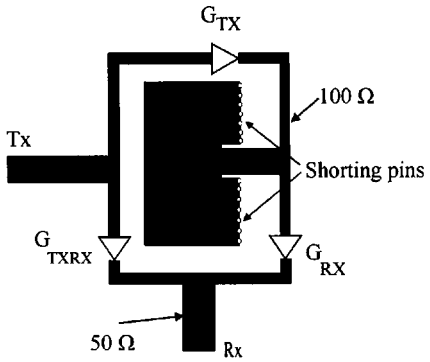

Fig. 4. Metal-surface layout of an integrated active circulator antenna based on 100-Ω gain blocks.

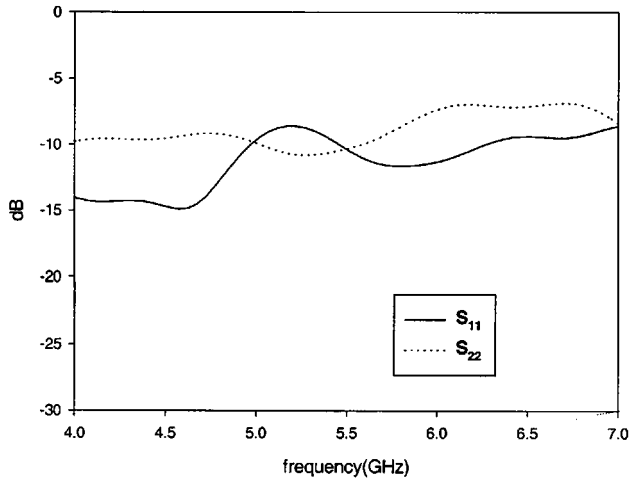

Fig. 5. Input and output S-parameters for active circulator antennas 100-Ω version (FDTD).

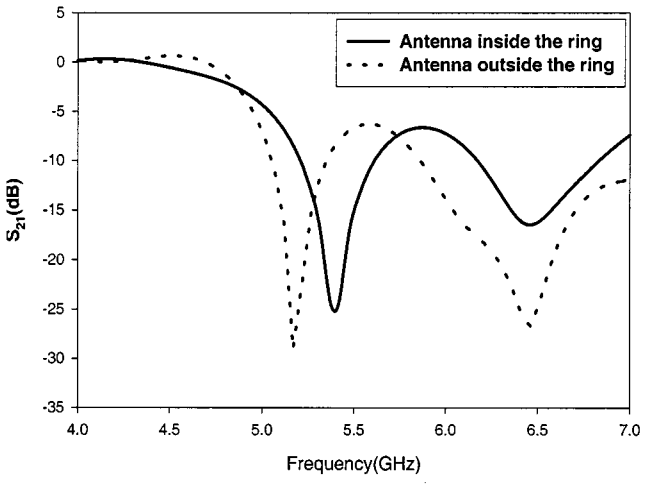

Fig. 6. Transmit and receive S-parameters for an active circulator antenna 100-Ω version (FDTD).

at the maximum isolation frequency reveals where the phase cancellation occurs (Fig. 3).

C. Integrated Active Circulator Antenna

The active circulator was integrated with a microstrip antenna to form a module with transmit–receive operation at the same frequency and polarization. A layout of the transceiver structure is shown in Fig. 4. A short-circuited inset-fed microstrip antenna is placed in the center of the ring to optimize the circuit area. Transmit–receive operation is possible by taking advantage of the isolation introduced by the circulator. Transmit power is amplified by gain block $G_{\rm TX}$ and coupled to the antenna port by a length of 50-Ω microstrip line. Receive power is coupled into the circulator via the same line and passes through $G_{\rm RX}$ since the reverse isolation of $G_{\rm TX}$ prevents power coupling back into the transmitter. The transceiver is linearly polarized with same polarization for transmit and receive.

D. FDTD Analysis of the Integrated Active Antenna Circulator

The FDTD code validated by the work in Section III-B was used to model the 100-Ω integrated configuration of Fig. 4. The antenna has a size of 8.5 × 15.6 mm, the inset length being 2.4 mm. Fig. 5 shows the simulated reflection coefficients at the transmit and receive ports. The effects of coupling within the structure were studied by comparing the simulated isolation when the antenna is positioned inside and outside of the ring structure (Fig. 6). The distributions of the fields when the antenna is inside (Fig. 7) and outside (Fig. 8) the ring reveal the cause of difference in the isolation. In the case where the antenna is inside the ring, the field is disrupted considerably, as indicated by the field maxima in the upper left-hand-side part of the circulator. The capability of examining effects of the antenna position relative to the circuit is a powerful feature of the extended FDTD method.

IV. Design Based on Commercial 50-Ω Gain Blocks

To realize the active circulator as a hybrid microwave integrated circuit, the only gain blocks readily available had nominal port impedances of 50 Ω. The S-parameters of one of the gain blocks (HP MGA-86 576) were measured at ten different bias levels to allow different gain settings. The circuit parameters,

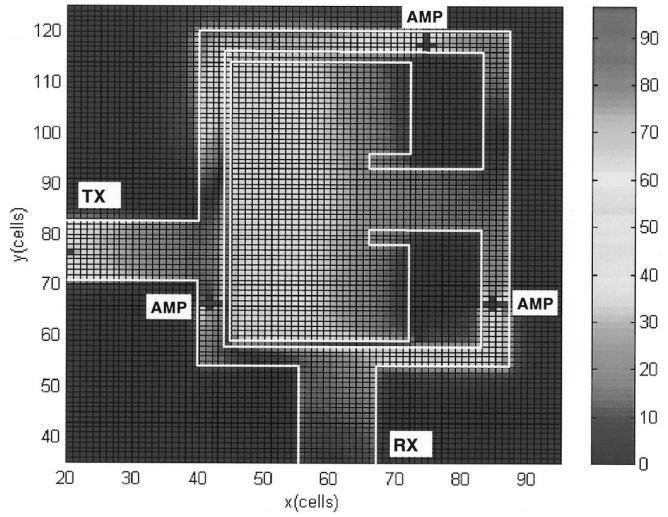

Fig. 7. Distribution of the normal electric-field magnitude on the surface for the active circulator antenna (100 Ω) when the antenna is placed inside the ring (calculated by FDTD). The space between white lines is metal and the rest is dielectric.

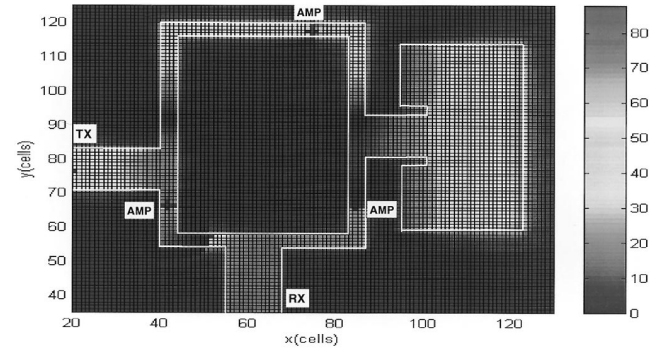

Fig. 8. Distribution of the normal electric-field magnitude on the surface for the active circulator antenna (100 Ω) when the antenna is placed outside the ring (calculated with FDTD). The space between white lines is metal and the rest is dielectric.

including the gain-block bias levels, were optimized for simultaneous isolation *and* matching. The gain of G_{TXRX} is set to the modeled value given by MDS and then fine tuned in the experimental hardware for maximum transmit/receive isolation. The whole circuit occupies less than 50 mm × 40 mm. The circuit is fully planar, with only dc-bias coils placed on the underside of the board. The 50-Ω circulator layout is shown in Fig. 9.

V. Experimental Evaluation of 50-Ω Gain-Block-Based Model

A. Circulator

The experimental model exhibits good transmit–receive isolation, which is predicted with reasonable accuracy from HP-MDS (Fig. 10). Circuit gains of approximately 6 and 3 dB in the transmit (S_{31}) and receive (S_{23}) paths, respectively, were measured at the maximum isolation frequency. This is an improvement from [8] where the use of nonreciprocal phase shifters was reported to obtain a similar cancellation effect, but with insertion loss present in all the signal paths. The return

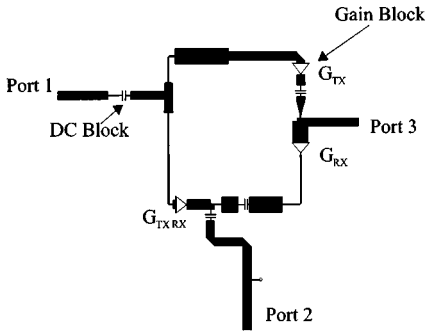

Fig. 9. Metal-surface layout of a planar active circulator based on commercial 50-Ω gain blocks.

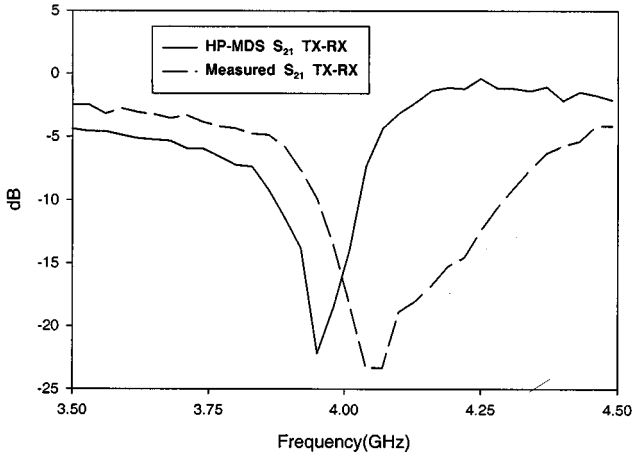

Fig. 10. Transmit–receive isolation (S_{21}) for a 50-Ω active circulator measured versus HP-MDS.

losses (S_{11}, S_{22}, S_{33}) were measured giving −10 dB at the maximum isolation frequency.

B. Integrated Antenna Circulator

The antenna used in the 50-Ω module (Fig. 11) measures 20 mm × 12 mm. Two open-circuit stubs have been used to match the antenna to the circulator. However, an optimized inset geometry would allow matching without the use of stubs. In Figs. 12 and 13, the S-parameters for the integrated active circulator antennas are presented. There is a noticeable difference between the transmit–receive isolation of the integrated structure (Fig. 13) and that of the nonintegrated circuit (Fig. 10). Instead of one dip, a double hump appears because of the interaction of the active circulator with the antenna. The introduction of the antenna, which is a resonant element, causes a small additional phase shift close to resonance. Thus, the condition of 180° phase difference can be fulfilled at another frequency, giving the second dip. The second dip is not at the operating frequency of the antenna. Section VII shows how the FDTD analysis can be used to study the effects of design dimensions on the position of the second dip, suggesting that it could be engineered to produce a more wide-band configuration. Nevertheless, the measured isolation is better than 20 dB over a 7-MHz band, with

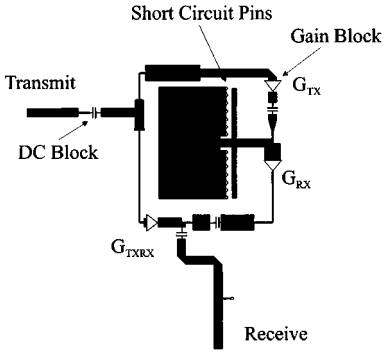

Fig. 11. Metal-surface layout of an integrated active circulator antenna based on commercial 50-Ω gain blocks.

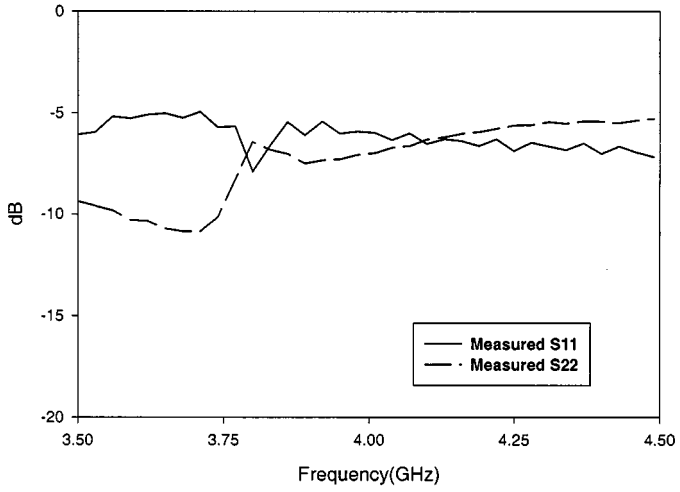

Fig. 12. Input and output S-parameters for 50-Ω active circulator antennas.

a maximum of 26.9 dB at 3.745 GHz where the antenna operates. The measured active antenna gains are seen to have larger bandwidths (Fig. 13), as have the return losses (Fig. 12). The gain of the short-circuit antenna has been measured separately as approximately 3 dBi. Thus, the circulator is adding approximately 4-dB gain on receive and 10-dB gain on transmit.

VI. Radiation Patterns for 50- and 100-Ω Structures

The radiation patterns for the 100-Ω active integrated antenna were calculated for the transmit case with the FDTD code [see Fig. 14(a)]. The transmit patterns for the 50-Ω structure were also measured [see Fig. 14(b)]. Near- to far-field transformation [13] was used to produce the radiation patterns. Observe that both the figures have essentially the same features. The cross-polar isolation was typically better than −10 dB at bore sight, as expected by the inherently poor cross-polar characteristics of a short-circuited patch. A significant characteristic of the radiation patterns is the off-axis dip of the H-plane cross-polar radiation pattern. In the case of a short-circuited patch, the dip is expected to be very close to boresight. In order to explain the translation of the dip, it is important to study Fig. 7. The skewness in the field distribution of the patch, introduced by the coupling, results in a shift in the cross-polar radiation pattern null.

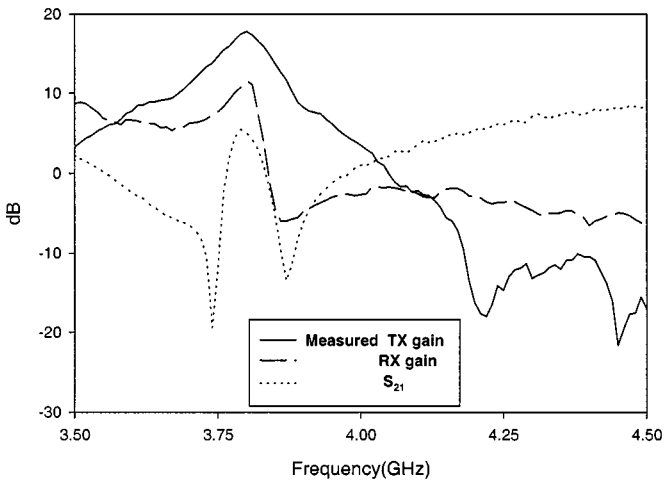

Fig. 13. Transmit and receive S-parameters for an active circulator antenna based on 50-Ω gain blocks (measured).

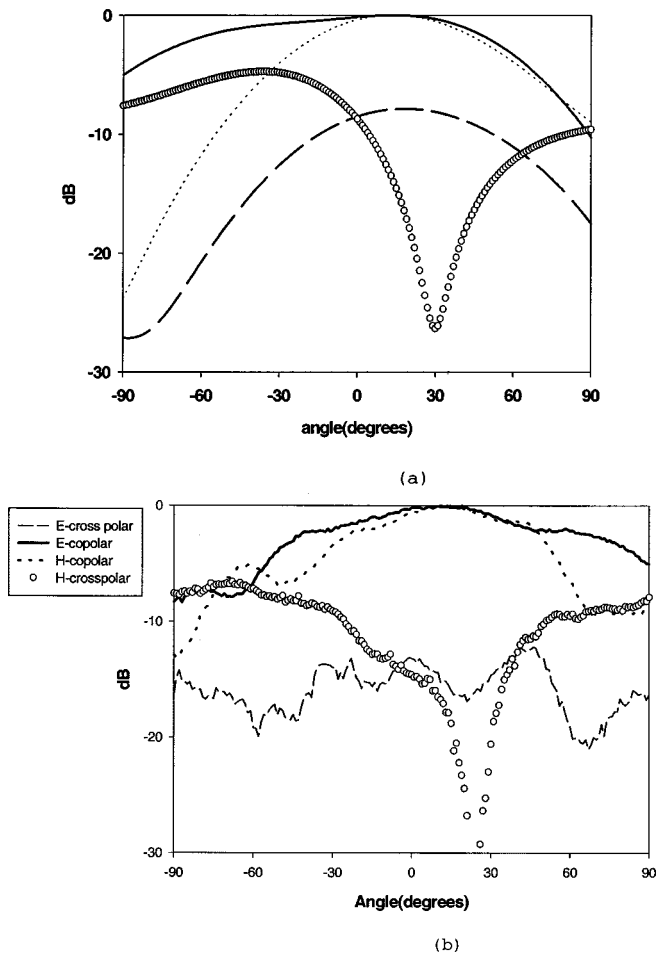

Fig. 14. Transmit radiation patterns for an active circulator antenna. (a) 100 Ω (FDTD). (b) 50-Ω structure (Measured).

VII. Design Considerations and Suggestions

From the previous sections, it is clear that the placement of the antenna inside the ring results in a compact module, but the performance (isolation, radiation patterns) is affected by the coupling. Obviously the coupling is controlled by the position of

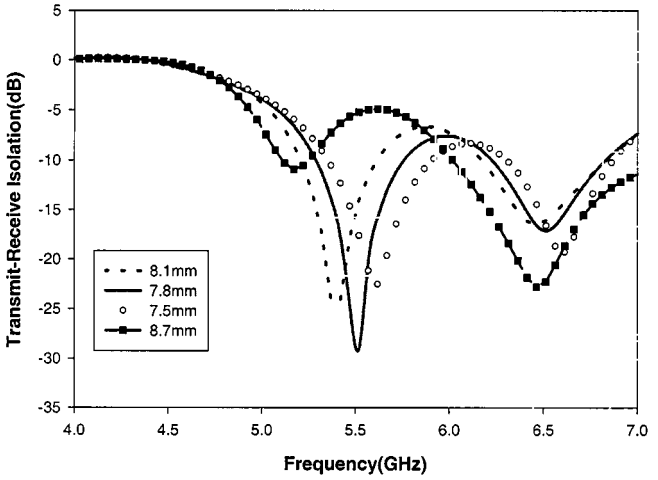

Fig. 15. Transmit–receive isolation with small variation of antenna length (100 Ω).

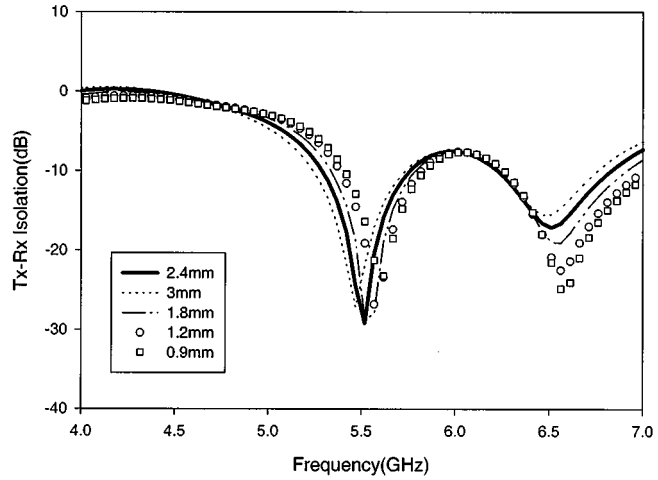

Fig. 16. Transmit–receive isolation with variation of inset (100 Ω).

the antenna relative to the circuit. Two parameters were varied in order to establish trends in the design of such modules.

The first parameter used is the size of the antenna. As explained in Section V, the circuit dip is shifted because of the antenna resonant behavior and coupling. The resonant frequency of small short-circuited antennas is affected by the diameter and number of shorting posts by 2%–3%, as Sanad [14] has demonstrated. Parametric investigations were performed by slightly varying the antenna length in order to optimize the isolation. In Fig. 15, the effect of the antenna size is demonstrated by plotting the transmit–receive isolation over the same frequency range for slightly different values of the length less than $\lambda_g/4$, which is 8.9 mm for operation at 5.6 GHz. For some value of the length that corresponds to a resonant frequency closer to the circulator dip, improved isolation can be achieved.

Another degree of freedom is the width of the antenna. By reducing the antenna width, coupling can be further reduced. From Fig. 6, it is clear that the absence of coupling results in isolation improvement by 5 dB. The gain degradation is compensated by the additional gain introduced by the gain blocks. The second parameter chosen is the inset length of the antenna feed that controls the input impedance of the antenna. For the optimized length of Fig. 15 ($L = 7.8$ mm), FDTD simulations were performed with different values of insets. From Fig. 16, it can be deduced that the frequency position of the dips is not strongly affected, but the isolation can be improved by a few decibels as the matching of the antenna changes.

The following trends, therefore, can be established using the FDTD method, enabling compactness to be achieved with predictable coupling.

- Antenna matching does not strongly affect the frequency where the dips occur, but can affect the isolation. Optimal matching for maximum isolation can be obtained.
- The best isolation can be achieved by producing an antenna that radiates at a frequency slightly higher than the frequency at which the maximum isolation of the circuit occurs.
- Increase in isolation can be further achieved by reduction of the antenna width.

VIII. Conclusion

The operation of an integrated active circulator antenna was discussed based on experimental results and results obtained from the application of the extended FDTD method. Arrays of these elements could overcome the power-handling problems that limit the performance of single elements. Undesired electromagnetic coupling is a crucial factor in the proper function of integrated-antenna circuit modules. By using FDTD, we demonstrated how the coupling affects the operation, providing explanations on observed experimental findings. Parametric calculations were also performed to establish design trends. By adjusting the size of the antenna and its input impedance, the isolation between transmit–receive can be controlled. The short-circuit quarter-wave patch antenna used in this paper has led to poor cross-polarization characteristics. In cases where high cross-polar isolation is required, FDTD analysis would be an ideal tool to assess the performance of alternative antenna choices. Design tools like FDTD with concurrent analysis capabilities are crucial to reduce costly prototype fabrication cycles.

References

[1] J. Lin and T. Itoh, "Active integrated antennas," *IEEE Trans. Microwave Theory Tech.*, vol. 42, pp. 2186–2194, Dec. 1994.

[2] M. J. Cryan, P. S. Hall, K. S. H. Tsang, and J. Sha, "Integrated active antenna with full duplex operation," *IEEE Trans. Microwave Theory Tech.*, vol. 45, pp. 1742–1748, Oct. 1997.

[3] M. J. Cryan and P. S. Hall, "Analysis of harmonic radiation from an active integrated antenna," *Electron. Lett.*, vol. 33, no. 24, pp. 1998–1999, 1997.

[4] W. Sui, D. A. Christensen, and C. H. Durney, "Extending the 2-D FDTD method to hybrid electromagnetic systems with active and passive lumped elements," *IEEE Trans. Microwave Theory Tech.*, vol. 40, pp. 724–730, Apr. 1992.

[5] M. Piket-May, A. Taflove, and J. Baron, "FDTD modeling of digital signal propagation in 3D circuits with passive and active loads," *IEEE Trans. Microwave Theory Tech.*, vol. 42, pp. 1514–1523, Aug. 1994.

[6] V. A. Thomas, K. Ling, M. E. Jones, B. Toland, and T. Itoh, "FDTD analysis of an active antenna," *IEEE Microwave Guided Wave Lett.*, vol. 4, pp. 296–298, Sept. 1994.
[7] Q. Chen and V. F. Fusco, "Time-domain diakoptics active slot ring antenna analysis using FDTD," in *Proc. 26th European Microwave Conf.*, Prague, Czech Republic, Sept. 9–12, 1996, pp. 440–443.
[8] S. Tanaka, N. Shimomura, and K. Ohtake, "Active circulators—The realization of circulators using transistors," *Proc. IEEE*, vol. 53, pp. 260–267, Mar. 1965.
[9] Y. Ayasli, "Field effect transistor circulators," *IEEE Trans. Magn.*, vol. 25, pp. 3242–3247, Sept. 1989.
[10] P. Katzin, Y. Ayasli, L. Reynolds, Jr., and B. Bedard, "6 to 18 GHz MMIC circulators," *Microwave J.*, pp. 248–256, May 1992.
[11] A. Reineix and B. Jecko, "Analysis of microstrip patch antennas using FDTD," *IEEE Trans. Antennas Propagat.*, vol. 37, pp. 1361–1369, Nov. 1989.
[12] G. Mur, "Absorbing boundary conditions for the finite difference approximation of the time domain electromagnetic field equations," *IEEE Trans. Electromag. Compat.*, vol. 23, pp. 377–382, Nov. 1981.
[13] R. J. Luebbers, K. S. Kunz, M. Schneider, and F. Hunsberger, "A finite difference time domain near-zone to far-zone transformation," *IEEE Trans. Antennas Propagat.*, vol. 39, pp. 429–433, Apr. 1991.
[14] M. Sanad, "Effect of shorting posts on short circuit microstrip antennas," in *IEEE AP-S Symp. Dig.*, 1994, pp. 794–797.

Christos Kalialakis was born in Watrellos, France, in 1971. He received the Ph.D. Degree in electronic and electrical engineering from The University of Birmingham, Birmingham, U.K., in 1999, and the B.Sc. in physics and the Master in telecommunications from the Aristotle University of Thessaloniki (A.U.Th), Thessaloniki, Greece, in 1993 and 1995, respectively.

During 1993, he was an undergraduate Research Assistant in the Department of Physics, A.U.Th., where he was involved with theoretical solid-state physics. From 1996 to 1998, he was a Postgraduate Teaching Assistant at the School of Electronic Engineering, The University of Birmingham. Since Nov. 1998, he has been a Research Associate at The University of Birmingham, where he is involved in an industry-sponsored project on satellite communications. His research interests include computational electromagnetics, active integrated antennas, and performance evaluation of mobile communications systems.

Dr. Kalialakis is an associate member of the Institute of Electrical Engineers (IEE), U.K., and a graduate member of the Institute of Physics, London, U.K.

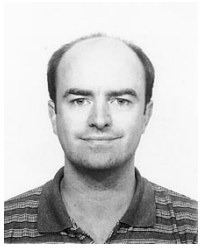

Martin J. Cryan (S'91–M'95) received the B.Eng. degree in electronic engineering from the University of Leeds, Leeds, U.K., in 1986, and the Ph.D. degree on the design and simulation of novel MMIC circuits and devices from the University of Bath, Bath, U.K., in 1994.

From 1986 to 1991, he worked in the microwave industry as a Microwave Design Engineer, where he was involved with diode detectors and waveguide products. In 1994, he assumed a Post-Doctoral position at The University of Birmingham, Birmingham, U.K., where he was involved with the design, simulation, and analysis of active integrated antennas. Since 1997, he has been a TMR Research Fellow at the University of Perugia, Perugia, Italy, where he is involved in the design and simulation of quasi-optical multipliers using the lumped-element FDTD method.

Peter S. Hall (M'88–SM'93) received the Ph.D. degree in antenna measurements from Sheffield University, Sheffield, U.K.

He then spent three years with Marconi Space and Defence Systems, Stanmore, U.K., where he was largely involved on a European Communications satellite project. He then joined The Royal Military College of Science, as a Senior Research Scientist, progressing to Reader in Electromagnetics. In 1994, he joined The University of Birmingham, Birmingham, U.K., where he is currently a Professor of communications engineering and Head of the Communications Engineering Group at the School of Electronic and Electrical Engineering. He has extensively researched the areas of microwave antennas, and associated components and antenna measurements. He has authored or co–authored four books and over 130 papers. He is currently on the Editorial Board of the *International Journal of RF and Microwave Computer Aided Engineering* and *Microwave and Optical Technology Letters*. He holds various patents.

Prof. Hall is a Fellow of the Institution of Electrical Engineers (IEE), U.K., a past chairman of the IEE Antennas and Propagation Professional Group and of the organizing committee of the 1997 IEE International Conference on Antennas and Propagation. He has been associated with the organization of many international conferences and is currently a member of the Technical Committee of AP200, Switzerland, and is an Overseas Corresponding Member of ISAP2000, Japan. He was honorary editor of *Proceedings IEE*, Part H, from 1991 to 1995. He has been awarded six IEE Premium Awards, including the 1990 IEE Rayleigh Book Award for the *Handbook of Microstrip Antennas*.

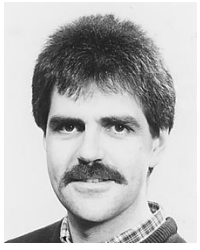

Peter Gardner (M'99) received the B.A. degree in physics from the University of Oxford, Oxford, U.K., in 1980, and the M.Sc. and Ph.D. degrees in electronic engineering, from the University of Manchester Institute of Science and Technology (UMIST), Manchester, U.K., in 1990 and 1992, respectively.

From 1981 to 1987, he was with Ferranti, Poynton, Cheshire, as a Senior Engineer involved with microwave amplifier development. From 1987 to 1989, he worked freelance in microwave engineering and software. In 1989, he joined the Department of Electrical Engineering and Electronics, UMIST, as a Research Associate, where he performed research in microwave negative resistance circuits, low-noise MMIC design, and tunable planar resonators. In 1994, he became a Lecturer at the School of Electronic and Electrical Engineering, The University of Birmingham, Birmingham, U.K. His current research interests are in the areas of microwave solid-state component design, active antennas, and amplifier linearization.